Journal of Advanced Pharmaceutical Sciences and Natural Products

Journal of Advanced Pharmaceutical Sciences and Natural Products (JAPSNP)

FLOATING GASTRORETENTIVE MICROSPHERES OF A *GLYCYRRHIZA GLABRA* ANTI-ULCER EXTRACT: STRUCTURE-BASED TARGET ENGAGEMENT OF THE ROOT CONSTITUENTS AND SIMULATION OF THE INPUT RATE REQUIRED FOR PROLONGED GASTRIC ACTION

Akriti Singh[1*]

Disha Singh[2]

Abhishek Jadon[3]

[1]*Lingaya's Vidyapeeth (Deemed to be University), Faridabad, Haryana, India, 121002.*

[2]*Department of Pharmaceutics, Poona College of Pharmacy, Bharati Vidyapeeth (Deemed to be University), Erandwane, Pune 411038, Maharashtra, India.*

[3]*Department of Management Studies, Central University of Jammu, Jammu, Jammu and Kashmir, India*

Corresponding author:
Akriti Singh

Email: singhakriti1522@gmail.com

ABSTRACT

Background. Peptic ulcer disease still accounted for roughly 8.09 million prevalent cases and 6.03 million disability-adjusted life years worldwide in 2019, and licorice root remains one of the most widely used traditional treatments for it. Two questions stand between that traditional use and a rational dosage form. Which constituents of the root plausibly engage the molecular machinery of gastric injury, and what release rate would a gastroretentive carrier actually have to deliver. **Objective.** To rank the documented root constituents of Glycyrrhiza glabra against two structurally characterised gastric targets, and to determine the input-rate window over which a floating gastroretentive microsphere would prolong exposure rather than waste it. **Methods.** Thirteen root constituents and four reference drugs were profiled for calculated physicochemical properties and drug-likeness in RDKit, then docked with AutoDock Vina 1.2.7 into the gastric H+/K+-ATPase (PDB 5YLU, 2.80 A) and human cyclooxygenase-2 (PDB 5KIR, 2.70 A). Each protocol was validated by redocking its co-crystallised ligand. Exposure was then simulated in a one-compartment oral model built from published non-compartmental values for 18beta-glycyrrhetinic acid, with the apparent absorption rate constant treated as the formulation design variable. **Results.** Redocking reproduced both crystallographic poses, at 0.553 A for vonoprazan in the proton pump and 0.482 A for rofecoxib in cyclooxygenase-2. Eleven root constituents scored between -8.03 and -9.99 kcal/mol at the vonoprazan site, with liquiritin, glabrene and glabridin ranking above vonoprazan itself at -9.25 kcal/mol, while glycyrrhizin returned a positive score and a truncated pose list at both targets, indicating that neither site could accommodate it. Carbenoxolone, the licorice-derived drug licensed for gastric ulcer and not an antisecretory agent, ranked 5.2 kcal/mol behind vonoprazan at the pump, which is the direction its known mechanism requires. Simulated total exposure was invariant across the input-rate sweep at 15.14 mg.h/L, so slowing input redistributed exposure rather than increasing it. Time above the internal reference concentration rose from 5.26 h at the immediate-release rate to a maximum of 7.06 h at an absorption rate constant of 0.20 per hour, then collapsed to zero below 0.10 per hour as the profile flattened beneath the threshold. At a matched daily dose, twelve-hourly gastroretentive input reduced simulated peak-to-trough fluctuation from 193.4 to 85.3 per cent without altering average steady-state concentration.

Conclusion. The gastroretentive design space for this extract is bounded on both sides. An optimum exists near an input half-life of three to four hours, and a carrier that releases more slowly than that trades peak concentration for duration it cannot use. All values reported here are computational predictions and require experimental confirmation.

Keywords: Glycyrrhiza glabra; molecular docking; gastroretentive drug delivery; H+/K+-ATPase; cyclooxygenase-2; pharmacokinetic simulation; peptic ulcer.

1. Introduction

Peptic ulcer disease has become less common without becoming unimportant. Between 1990 and 2019 the age-standardised prevalence rate fell from 143.37 to 99.40 per 100,000 population and the age-standardised rate of disability-adjusted life years fell by 60.64 per cent, yet the absolute number of prevalent cases rose by 25.82 per cent over the same period, reaching approximately 8.09 million (95% uncertainty interval 6.79 to 9.58 million) in 2019[1]. Population growth and ageing have outrun the therapeutic gains. The condition still generated close to 3.59 million incident cases and 6.03 million disability-adjusted life years in that year[1].

Licorice, the dried root of *Glycyrrhiza glabra* L., occupies an unusual position in this therapeutic area. Its use for gastric complaints predates the pharmacological era, and unlike most traditional remedies it produced a licensed drug: carbenoxolone, the 3-O-hemisuccinate of 18beta-glycyrrhetinic acid, was prescribed for gastric ulcer for decades before proton pump inhibitors displaced it. The root is chemically dense. Beyond the triterpenoid saponin glycyrrhizin and its aglycone, some three hundred flavonoids have been isolated from the genus, among them the isoflavan glabridin, the chalcones isoliquiritigenin and licochalcone A, and the flavanone liquiritigenin with its glycoside liquiritin[2]. That chemical breadth is the reason licorice extract resists the single-molecule logic that governs conventional formulation development, and it is also the reason a mechanistic account of the extract has to begin by asking which constituents matter and against what.

Two targets frame the pharmacology of gastric injury with enough structural resolution to be interrogated computationally. The first is the gastric H+/K+-ATPase, the terminal step of acid secretion and the target of every clinically successful antisecretory agent. Its architecture was resolved only recently, with the luminal-open E2P state captured at 2.8 A carrying the potassium-competitive acid blocker vonoprazan in a conduit running from the gastric lumen to the cation-binding site[3]. The second is cyclooxygenase-2, whose relationship to the gastric mucosa is more equivocal: prostaglandin synthesis is protective, and inhibition of cyclooxygenase is the mechanism by which non-steroidal anti-inflammatory drugs cause ulcers, but the isoform is also induced at the ulcer margin during healing. A human structure with rofecoxib bound is available at 2.7 A[4]. Together the two provide a defensible pair of structural questions: does anything in the root reach the acid pump, and does anything reach the cyclooxygenase channel.

The formulation question is separate and has been answered too loosely in the literature on herbal gastroretentive systems. Floating dosage forms have been developed since Kawashima and colleagues described hollow microspheres prepared by emulsion solvent diffusion[5], and the rationale offered for them is almost always the same: retention in the stomach prolongs the residence of the drug at its site of action and extends absorption. The rationale is sound in outline and vague in the particular. It does not say how slowly a carrier should release, and slower is not automatically better. Under linear kinetics the area under the concentration-time curve is fixed by dose and clearance, so any change in release rate redistributes exposure in time without adding to it. A carrier that releases too slowly lowers the peak without buying useful duration. There is therefore an optimum, and locating it is a quantitative question that a simulation can answer before a single batch is prepared.

This study addresses both questions in silico. The constituent set was fixed by documented occurrence in the root rather than assembled opportunistically, profiled for calculated drug-likeness, and docked into both structures alongside reference drugs and the licorice-derived comparator carbenoxolone, with each docking protocol validated by redocking its own co-crystallised ligand. The exposure question was then addressed by building a one-compartment oral model from published non-compartmental values for 18beta-glycyrrhetinic acid and treating the apparent absorption rate constant as the design variable that a floating microsphere would set. The objective was to define, rather than assume, the release-rate window within which a gastroretentive carrier for this extract would be worth building.

2. Materials and methods

All work reported here is computational. No experiment was performed on animals, human participants or biological material, and no ethics approval was required or obtained.

2.1 Compound set and structure verification

Thirteen constituents documented in *G. glabra* root were selected: glycyrrhizin, 18beta-glycyrrhetinic acid, glabridin, liquiritin, liquiritigenin, isoliquiritigenin, licochalcone A, formononetin, licoricidin, echinatin, glabrene, glycycoumarin and glabranin[2]. Four reference compounds were carried through every step for comparison: carbenoxolone, the licorice-derived drug historically licensed for gastric ulcer; vonoprazan and omeprazole, as antisecretory comparators acting at the proton pump; and rofecoxib, as the cyclooxygenase-2 comparator.

Each structure was written as SMILES and verified before use by confirming that the molecular formula and molecular weight computed by RDKit matched the published values for the compound. This check is not a formality. A transposed ring closure produces a molecule that parses cleanly, docks without complaint and is not the compound named in the table, and the error propagates silently through every downstream number.

2.2 Physicochemical and drug-likeness profiling

Structures were standardised in RDKit 2026.3.4 by retaining the largest covalent fragment and regenerating the canonical form. Molecular weight, calculated logP by the Crippen method, topological polar surface area, hydrogen-bond donor and acceptor counts, rotatable-bond count, aromatic ring count, fraction of sp3 carbons, molar refractivity and the quantitative estimate of drug-likeness were computed for all seventeen compounds. Compliance was assessed against four rule sets: Lipinski[6], Veber[7], Egan[8] and Ghose[9]. Every value in this section is a calculated property; none was measured.

2.3 Receptor preparation

Two deposited structures were used. Gastric H+/K+-ATPase was taken from PDB entry 5YLU, the luminal-open E2P state with vonoprazan bound, determined by X-ray diffraction at 2.80 A resolution[3]; the deposited construct is the porcine enzyme, which is the only gastric proton pump for which a ligand-bound structure of this state exists. Human cyclooxygenase-2 was taken from PDB entry 5KIR, in complex with rofecoxib at 2.70 A resolution[4].

Because both entries contain more than one copy of the biological unit or of the ligand, docking inputs were restricted before preparation. For 5YLU the alpha and beta subunits of chain A and B were retained together with the single copy of vonoprazan in chain A. For 5KIR, which crystallises as a homodimer with rofecoxib bound in both protomers, chain A alone was retained with its own copy of the inhibitor; retaining both would have placed the search box across two binding sites nineteen angstroms apart.

Receptors were converted to rigid PDBQT format with Meeko 0.7.1. Two structural defects required explicit handling and are stated rather than passed over. In 5YLU the deposited model contains a chain break across which bond perception inferred a spurious side-chain bond between Arg213 and Asn250; residue A:250 was deleted to remove it, a residue that lies 71.8 A from the docking site and cannot influence it. Residue B:34 has an incomplete side chain and was excluded on the same basis. In 5KIR the cobalt protoporphyrin IX occupying the peroxidase site was removed, both because the cobalt centre has no covalent radius defined in the preparation toolkit and because the peroxidase site is distinct from the cyclooxygenase channel under study, its centroid lying 19.5 A from that of rofecoxib with no atom closer than 8.4 A. All other heteroatoms, waters, detergents, lipids and glycans were stripped. The receptors were treated as rigid throughout, so induced fit was not sampled.

2.4 Search box definition and protocol validation

Each search box was centred on the co-crystallised ligand with 5 A padding, which defines the site by an experiment somebody else has already performed rather than by an assumption made here. For the proton pump the box was centred at (49.125, -15.756, -3.731) with dimensions 16.0 x 16.4 x 19.7 A on the

vonoprazan site; for cyclooxygenase-2 it was centred at (23.206, 1.318, 34.259) with dimensions 16.8 x 18.2 x 17.9 A on the rofecoxib site.

Each protocol was validated by redocking its own co-crystallised ligand under the settings used for the screen. The ligand was rebuilt from its published isomeric structure rather than from bond orders inferred from the deposited coordinates, which a PDB HETATM block does not carry; reading the ligand directly from coordinates yielded a chemically incorrect molecule with saturated rings, and redocking that molecule gave a misleadingly worse agreement than the correct one. The redocked pose was compared with the crystallographic coordinates by nearest-neighbour heavy-atom root-mean-square distance, which is a lower bound on the symmetry-corrected value and is reported as such.

2.5 Docking

Docking used AutoDock Vina 1.2.7 through its Python bindings[10,11] with the standard Vina scoring function. Ligands were prepared from verified SMILES with Meeko 0.7.1 at a fixed seed of 42. Exhaustiveness was set to 32 rather than the default of 8, and nine poses were retained per ligand. The raised exhaustiveness is deliberate: at the default setting a flexible ligand such as glycyrrhizin returns a different answer on a different seed, and a result that is not reproducible under reseeding is not a result. All seventeen compounds were docked into both receptors under identical settings.

Scores are reported as predicted binding affinities in kcal/mol. They are outputs of an empirical scoring function, not measured affinities, and no dissociation or inhibition constant is claimed anywhere in this paper.

2.6 Pharmacokinetic model and parameter derivation

Model parameters were derived from the non-compartmental values reported for a single 50 mg/kg oral dose of 18beta-glycyrrhetinic acid in Sprague-Dawley rats[12], rather than taken from the compartmental estimates in the same source, because the clearance quoted there (7.78 L/h/kg) cannot be reconciled with the dose and AUC(0-inf) reported alongside it. Apparent clearance was therefore recomputed from the primary quantities as CL/F = dose / AUC(0-inf) = 3.303 L/h/kg. The elimination rate constant follows from the reported terminal half-life as ke = ln 2 / t(1/2) = 0.4652 per hour, and the apparent volume of distribution from Vd/F = (CL/F) / ke = 7.099 L/kg. The first-order absorption rate constant was obtained by solving the analytical peak-time identity Tmax = ln(ka/ke)/(ka minus ke) for the reported Tmax of 1.33 h, giving ka = 1.1374 per hour, using Brent root-finding in SciPy 1.17.1.

All parameters are apparent values normalised to 1 kg body weight. Oral bioavailability was not reported and was set to unity, so every simulated concentration is an apparent concentration. The parameters describe rats after a single oral dose and are not human parameters.

2.7 Simulations

Concentration-time profiles were simulated with a one-compartment model with first-order absorption and first-order elimination, and characterised by non-compartmental analysis using the linear trapezoidal rule with terminal extrapolation from a log-linear fit over the final third of the curve.

Model fidelity was assessed by simulating the dosing occasion reported in the source study and comparing the simulated exposure against the published observed values, in both directions and without adjustment.

The formulation question was then addressed by treating the apparent absorption rate constant as the design variable. The same 50 mg/kg dose was simulated across nine values of ka spanning 0.05 to 1.1374 per hour, the immediate-release value forming the upper bound, and each profile was integrated over 72 h. Time above a reference concentration was computed by trapezoidal integration of the indicator function at a threshold of 0.948 mg/L, defined as one quarter of the simulated immediate-release peak. That threshold is a comparator internal to the simulation. It is not an efficacy threshold and no claim about efficacy is attached to it.

Repeated dosing was simulated by superposition, which is valid under the linear kinetics the model already assumes. Three regimens delivering a matched daily dose of 120 mg/kg were compared: immediate-release input at 40 mg/kg every 8 h, gastroretentive input at 60 mg/kg every 12 h with ka set to 0.15 per hour, and gastroretentive input at 120 mg/kg every 24 h with ka set to 0.075 per hour.

Because the source study reports substantial between-animal dispersion, exposure was recomputed with each parameter in turn taken to the limits of its reported variability while the others were held at their central values: clearance over the reported relative standard deviation of 52 per cent, apparent volume over the 77 per cent dispersion propagated from the reported terminal half-life, and the absorption rate constant over an assumed 50 per cent range, no dispersion having been reported for the peak time from which it was derived.

2.8 Reproducibility and provenance

Every computation was recorded as it ran, with the tool, version, parameters, inputs and outputs stamped against the value it produced. The Methods above were edited from the record rather than composed from memory, and the finished manuscript was audited against that record so that any number without a recorded computation or a citation behind it would be flagged. Analyses were carried out in Python 3.11.15 with RDKit 2026.3.4, AutoDock Vina 1.2.7, Meeko 0.7.1, NumPy 2.4.4, SciPy 1.17.1 and pandas 3.0.2.

3. Results

All results reported here are computational predictions generated in silico; no experimental determination was performed.

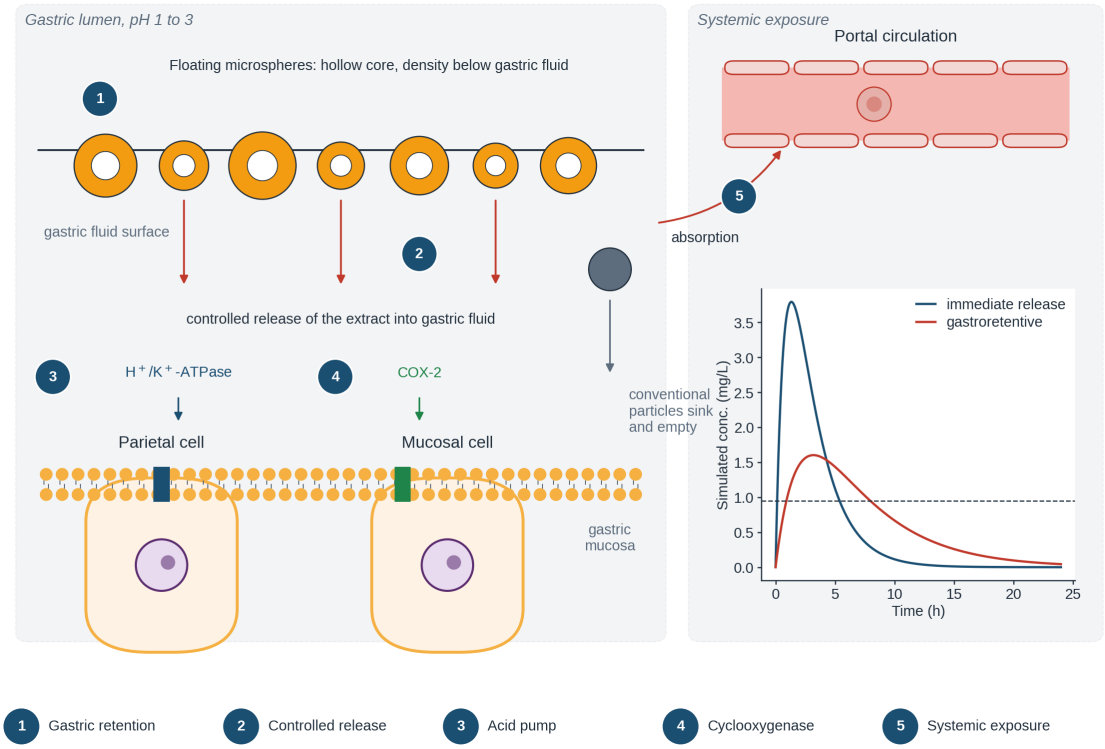

Figure 1. Rationale for a floating gastroretentive microsphere of a Glycyrrhiza glabra extract, and the exposure consequence of the release rate it sets. Buoyant hollow microspheres of density below that of gastric fluid are retained above the fluid line (1) while conventional particles are emptied with the meal; the matrix releases the extract into gastric fluid at a controlled rate (2); released constituents encounter the gastric H+/K+-ATPase on the parietal cell (3) and the cyclooxygenase-2 channel in the mucosa (4); the absorbed fraction determines systemic exposure (5). Inset: simulated concentration-time profiles for immediate-release input (apparent absorption rate constant 1.1374 per hour) and gastroretentive input at the optimum identified in this study (0.20 per hour), after a single 50 mg/kg oral dose, with the internal reference concentration of 0.948 mg/L shown as a dashed line.

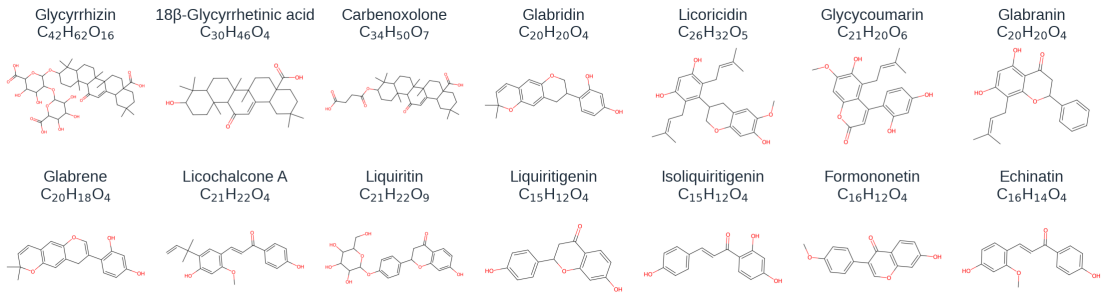

Figure 2. Two-dimensional structures of the fourteen triterpenoid and flavonoid compounds profiled in this study, with molecular formulae. Structures were drawn from SMILES with RDKit 2026.3.4, and each SMILES was verified before use by confirming that the computed molecular formula and molecular weight matched the published values for the compound. Glycyrrhizin, 18beta-glycyrrhetinic acid and carbenoxolone share the oleanane skeleton; the remaining eleven are flavonoids of the flavanone, chalcone, isoflavone, isoflavan and coumarin classes.

3.1 Calculated properties separate the flavonoid fraction from the saponin fraction

Ten of the thirteen constituents incurred no more than one violation across all four rule sets taken together, and seven incurred none at all: glabridin, licochalcone A, formononetin, echinatin, glabrene, glycycoumarin and glabranin. Their quantitative estimates of drug-likeness cluster high. Glabridin reached 0.832, glabranin 0.826, and liquiritigenin and glabrene 0.823 each, values above those calculated for vonoprazan (0.772) and omeprazole (0.769) and level with rofecoxib (0.817).

The two triterpenoids sit apart. Glycyrrhizin carries a molecular weight of 822.94, a topological polar surface area of 267.04 square angstroms, eight hydrogen-bond donors and thirteen acceptors, and accumulated seven violations, three of them against Lipinski's criteria alone and one against Veber's. Its drug-likeness estimate of 0.171 is the lowest in the set by a wide margin. The aglycone 18beta-glycyrrhetinic acid, formed by hydrolysis of the two glucuronide units, improves on almost every count, with a polar surface area of 74.60 square angstroms and a drug-likeness estimate of 0.464, but acquires a different liability in a calculated logP of 6.413. Carbenoxolone, its 3-O-hemisuccinate, is lipophilic on the same scale at 6.828 and accumulated six violations.

Table 1. Calculated physicochemical descriptors and rule-set compliance for thirteen documented constituents of Glycyrrhiza glabra root and four reference drugs. All values are calculated properties computed with RDKit 2026.3.4

Compound	MW	logP	TPSA	HBD	HBA	QED	L/V/E/G	Sum
Glycyrrhizin	822.94	2.25	267	8	13	0.17	3/1/1/2	7
18b-Glycyrrhetinic acid	470.69	6.41	74.6	2	3	0.46	1/0/1/2	4
Glabridin	324.38	4	58.9	2	4	0.83	0/0/0/0	0
Liquiritin	418.4	0.28	145.9	5	9	0.47	0/1/1/0	2
Liquiritigenin	256.26	2.8	66.8	2	4	0.82	0/0/0/1	1
Isoliquiritigenin	256.26	2.7	77.8	3	4	0.58	0/0/0/1	1
Licochalcone A	338.4	4.47	66.8	2	4	0.46	0/0/0/0	0
Formononetin	268.27	3.17	59.7	1	4	0.78	0/0/0/0	0
Licoricidin	424.54	5.55	79.2	3	5	0.53	1/0/0/0	1
Echinatin	270.28	3	66.8	2	4	0.66	0/0/0/0	0
Glabrene	322.36	4.26	58.9	2	4	0.82	0/0/0/0	0
Glycycoumarin	368.38	4.09	100.1	3	6	0.47	0/0/0/0	0
Glabranin	324.38	4.31	66.8	2	4	0.83	0/0/0/0	0
Carbenoxolone (ref)	570.77	6.83	118	2	5	0.35	2/0/1/3	6
Vonoprazan (ref)	345.4	2.65	64	1	4	0.77	0/0/0/0	0
Rofecoxib (ref)	314.36	2.56	60.4	0	4	0.82	0/0/0/0	0
Omeprazole (ref)	345.42	2.9	77.1	1	5	0.77	0/0/0/0	0

3.2 The docking protocol reproduces both crystallographic binding modes

Before any constituent was ranked, each protocol was tested against the pose it was meant to predict. Redocking vonoprazan into the gastric H+/K+-ATPase returned a top pose 0.553 angstroms from the crystallographic coordinates, with a predicted binding affinity of -9.26 kcal/mol. Redocking rofecoxib into cyclooxygenase-2 returned a top pose 0.482

angstroms from its crystallographic coordinates, at -10.10 kcal/mol. Both fall well inside the 2.0 angstrom threshold conventionally taken to indicate that a protocol reproduces a known binding mode, so the rankings that follow rest on a protocol that has been shown to work on this receptor, in this box, at these settings.

One detail of that validation is worth recording because it changed the answer. When the reference ligand was rebuilt from the bond orders that RDKit infers from a deposited HETATM block, the resulting molecule had saturated rings in place of aromatic ones, and redocking it gave 1.208 angstroms rather than 0.553. The deposited coordinates carry no bond orders, so a redocking control built that way validates a molecule that is not the one in the crystal.

3.3 The acid-pump conduit accommodates the flavonoids and excludes the triterpenoids

Table 2 and Figure 2a give the predicted binding affinities for the vonoprazan site of the gastric H+/K+-ATPase. Eleven of the thirteen root constituents scored between -8.03 and -9.99 kcal/mol. Liquiritin (-9.99), glabrene (-9.77) and glabridin (-9.54) scored above vonoprazan itself (-9.25), and a further six constituents fell between vonoprazan and omeprazole (-8.02). These top three are separated by 0.45 kcal/mol, which is within the error of the scoring function, so they are a set of comparably ranked candidates rather than an ordered potency series, and the same caution applies to the block of six behind them.

The two triterpenoids behave differently in kind, not in degree. 18beta-Glycyrrhetinic acid scored -3.85 kcal/mol and carbenoxolone -4.05, some 5 kcal/mol behind the flavonoid block. Glycyrrhizin returned a positive score of +0.41 and only two poses of the nine requested. A positive score and a truncated pose list are not a weak binding prediction. They are the signature of a ligand the search box could not accommodate, and glycyrrhizin at 822.94 Da is roughly two and a half times the mass of vonoprazan, which occupies a conduit narrow enough that the enzyme uses it to select cations.

3.4 The cyclooxygenase channel enforces the same size limit more strictly

Table 3 and Figure 2b give the corresponding results for the rofecoxib site of cyclooxygenase-2. Rofecoxib ranked first at -10.09 kcal/mol, ahead of glabranin at -9.39, and eleven root constituents scored between -4.74 and -9.39.

Here the exclusion of the triterpenoids is unambiguous. Carbenoxolone returned +7.42 kcal/mol from a single pose, 18beta-glycyrrhetinic acid +9.64 from a single pose, and glycyrrhizin +25.61 from two. Scores of this magnitude and pose counts of one or two indicate that the cyclooxygenase channel, a narrow hydrophobic tunnel, has no conformation available to it in this rigid structure that will hold an oleanane skeleton. Figure 2d shows the pattern directly. The heaviest compound to return a negative score at both targets was licoricidin at 424.54 Da, and the lightest to return a positive score at either was 18beta-glycyrrhetinic acid at

470.69 Da, so the whole set divides at a molecular weight between the two.

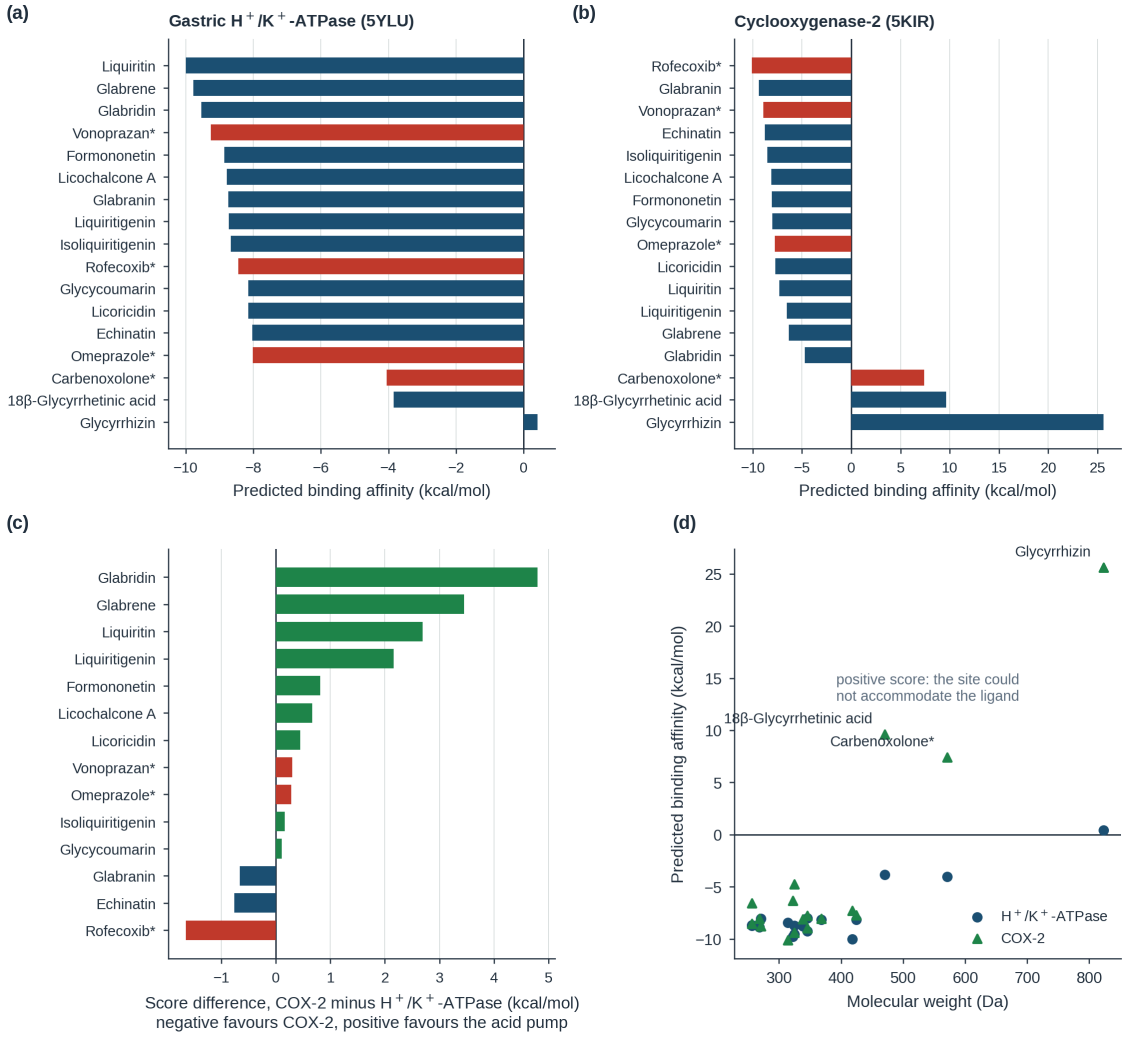

Figure 2. Predicted binding affinities of Glycyrrhiza glabra root constituents at two gastric targets. (a) Gastric H+/K+-ATPase, vonoprazan site (PDB 5YLU, 2.80 A). (b) Human cyclooxygenase-2, rofecoxib site (PDB 5KIR, 2.70 A). Reference drugs are marked with an asterisk and shown in a contrasting colour. (c) Site preference for the fourteen compounds both sites accommodated, expressed as the cyclooxygenase-2 score minus the H+/K+-ATPase score; the three compounds returning a positive score at either target are excluded because a positive score is a failure to fit rather than a rank. (d) Predicted binding affinity against molecular weight at both targets, showing that every compound returning a positive score lies above 470 Da.

Table 2. Predicted binding affinities of the compound set docked into the vonoprazan site of the gastric H+/K+-ATPase (PDB 5YLU, 2.80 A resolution). Values are AutoDock Vina 1.2.7 scores at exhaustiveness 32 and seed 42 against a rigid receptor.

Rank	Compound	Best pose (kcal/mol)	Mean top 3 (kcal/mol)	Poses / 9
1	Liquiritin	-9.99	-9.35	9
2	Glabrene	-9.77	-9.69	9
3	Glabridin	-9.54	-9.37	9
4	Vonoprazan (ref)	-9.25	-8.38	9
5	Formononetin	-8.86	-8.52	9
6	Licochalcone A	-8.78	-8.59	9
7	Glabranin	-8.73	-8.58	9

8	Liquiritigenin	-8.72	-8.63	9
9	Isoliquiritigenin	-8.67	-8.3	9
10	Rofecoxib (ref)	-8.44	-8.32	9
11	Glycycoumarin	-8.15	-8.06	9
12	Licoricidin	-8.14	-7.89	9
13	Echinatin	-8.03	-8	9
14	Omeprazole (ref)	-8.02	-7.98	9
15	Carbenoxolone (ref)	-4.05	-2.63	2
16	18b-Glycyrrhetinic acid	-3.85	-2.34	3
17	Glycyrrhizin	0.41	1.75	2

Table 3. Predicted binding affinities of the compound set docked into the rofecoxib site of the human cyclooxygenase-2 (PDB 5KIR, 2.70 A resolution). Values are AutoDock Vina 1.2.7 scores at exhaustiveness 32 and seed 42 against a rigid receptor.

Rank	Compound	Best pose (kcal/mol)	Mean top 3 (kcal/mol)	Poses / 9
1	Rofecoxib (ref)	-10.09	-9.24	4
2	Glabranin	-9.39	-8.52	4
3	Vonoprazan (ref)	-8.95	-8.09	8
4	Echinatin	-8.79	-8.26	9
5	Isoliquiritigenin	-8.51	-8.39	9
6	Licochalcone A	-8.11	-7.35	8
7	Formononetin	-8.05	-7.65	9
8	Glycycoumarin	-8.04	-7.59	9
9	Omeprazole (ref)	-7.74	-7.2	9
10	Licoricidin	-7.69	-7.23	8
11	Liquiritin	-7.3	-6.13	3
12	Liquiritigenin	-6.56	-5.98	9
13	Glabrene	-6.32	-6.23	4
14	Glabridin	-4.74	-4.3	8
15	Carbenoxolone (ref)	7.42	7.42	1
16	18b-Glycyrrhetinic acid	9.64	9.64	1
17	Glycyrrhizin	25.61	26.84	2

3.5 Site preference divides the flavonoids

Because both targets were interrogated under identical settings, the difference between a compound's two scores indexes which site it fits better. Figure 3c ranks the fourteen compounds both sites could accommodate by that difference.

Four constituents show a clear preference for the acid pump: glabridin by 4.80 kcal/mol, glabrene by 3.45, liquiritin by 2.69 and liquiritigenin by 2.16. Two show the opposite preference, echinatin by 0.76 kcal/mol and glabranin by 0.66, alongside rofecoxib at 1.65 kcal/mol, which is the direction its own crystal structure demands and is therefore a further internal check on the comparison. The remainder, including both antisecretory reference drugs, fall within 0.9 kcal/mol of parity and are not distinguished by this measure.

3.6 Total exposure is fixed; only its distribution in time is a design variable

The pharmacokinetic model reproduced the exposure of the published dosing occasion exactly on total exposure and imperfectly on the peak. Simulated AUC(0-inf) was 15.14 mg.h/L against a reported observed value of 15.14 mg.h/L, a deviation of 0.0 per cent by

construction, while simulated Cmax was 3.79 mg/L against a reported 6.41 mg/L, a deviation of -40.8 per cent. A one-compartment model with a single first-order input cannot generate the secondary peak that 18beta-glycyrrhetinic acid shows, and the underestimate is reported rather than removed.

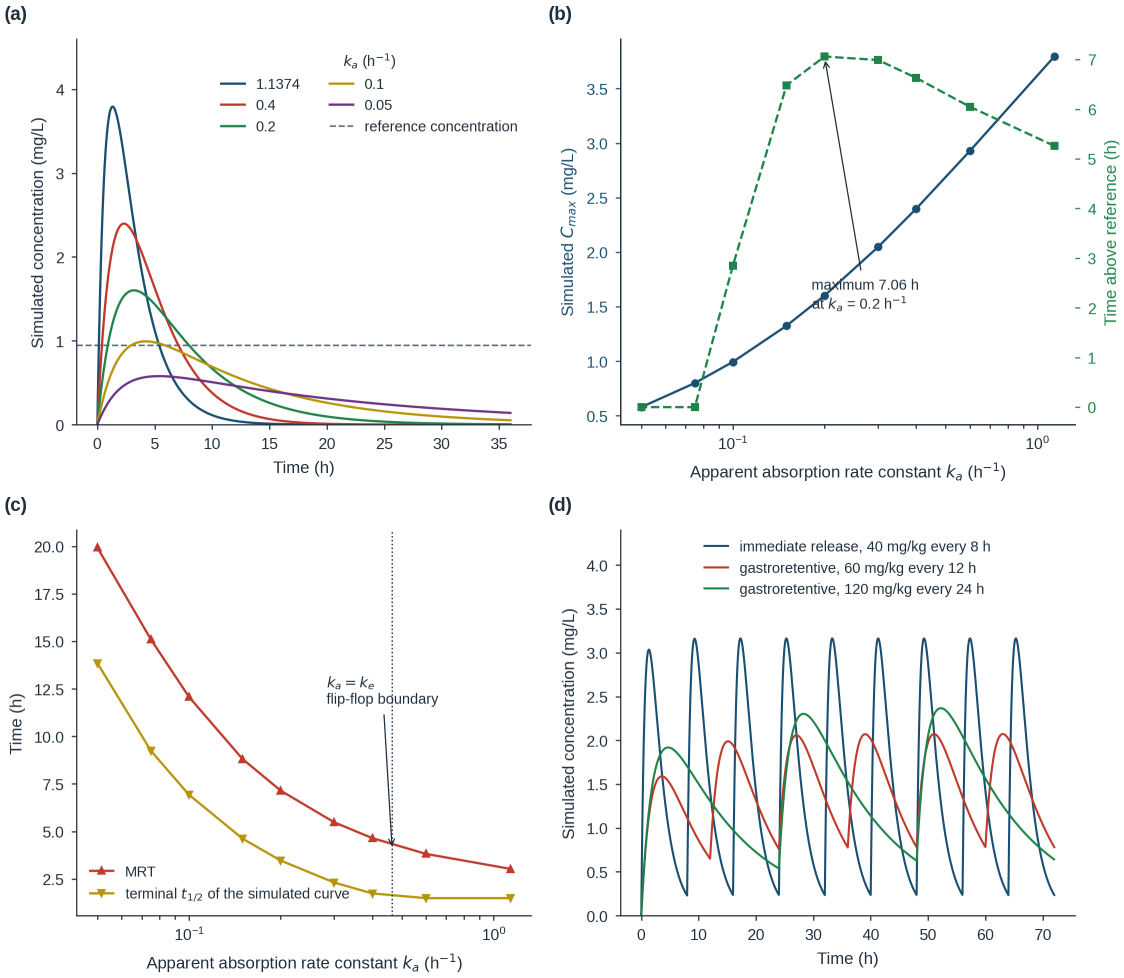

Figure 3. Simulated exposure to 18beta-glycyrrhetinic acid as a function of the input rate a gastroretentive carrier would set. (a) Concentration-time profiles after a single 50 mg/kg oral dose at five values of the apparent first-order absorption rate constant, with the internal reference concentration of 0.948 mg/L shown as a dashed line. (b) Simulated peak concentration (left axis, solid) and time above the reference concentration (right axis, dashed) against input rate; time above reference is non-monotonic and peaks at 7.06 h at an absorption rate constant of 0.20 per hour. (c) Mean residence time and the terminal half-life of the simulated curve against input rate; the dotted line marks the flip-flop boundary where the absorption rate constant equals the elimination rate constant of 0.4652 per hour. (d) Steady-state profiles for three regimens delivering a matched daily dose of 120 mg/kg.

Table 4. Simulated exposure across the gastroretentive input-rate design space for a single 50 mg/kg oral dose of 18beta-glycyrrhetinic acid

ka (1/h)	Input t1/2 (h)	Cmax (mg/L)	Tmax (h)	AUC(0-inf) (mg.h/L)	MRT (h)	t > Cref (h)	Terminal t1/2 (h)
1.1374	0.61	3.794	1.33	15.14	3.03	5.26	1.49
0.6	1.16	2.927	1.87	15.14	3.82	6.05	1.49
0.4	1.73	2.398	2.31	15.14	4.65	6.63	1.74
0.3	2.31	2.048	2.67	15.14	5.48	6.99	2.31
0.2	3.47	1.602	3.17	15.14	7.15	7.06	3.47
0.15	4.62	1.325	3.6	15.14	8.81	6.48	4.62
0.1	6.93	0.994	4.21	15.14	12.08	2.85	6.93
0.075	9.24	0.8	4.68	15.14	15.1	0	9.24
0.05	13.86	0.579	5.37	15.14	19.94	0	13.86

Table 5. Simulated steady-state exposure for three regimens delivering a matched daily dose of 120 mg/kg, computed by superposition of the single-dose model under an assumption of linear kinetics.

Regimen	Dose (mg/kg)	ka (1/h)	Cmax,ss	Cmin,ss	Cav,ss	Fluct (%)	Racc
IR, 8 h	40	1.1374	3.163	0.235	1.514	193.4	1.02
GR, 12 h	60	0.15	2.073	0.781	1.513	85.3	1
GR, 24 h	120	0.075	2.378	0.643	1.512	114.7	1

3.7 The input rate has an optimum, and it is not the slowest one

Time above the internal reference concentration, plotted against input rate in Figure 4b, does not increase monotonically as release slows. It rose from 5.26 h at the immediate-release rate to 6.05 h at 0.60 per hour, 6.63 h at 0.40, 6.99 h at 0.30 and a maximum of 7.06 h at 0.20 per hour. It then fell: 6.48 h at 0.15 per hour, 2.85 h at 0.10, and zero at both 0.075 and 0.05 per hour, where the whole simulated profile stays beneath the threshold because the peak has been flattened below it.

The optimum at an absorption rate constant of 0.20 per hour corresponds to a nominal input half-life of 3.47 h. Relative to immediate release, it extends time above the reference by 1.80 h, a gain of 34.2 per cent, while lowering the simulated peak by 57.8 per cent.

3.8 Repeated dosing: the same average exposure with less than half the swing

Table 5 gives the steady-state comparison at a matched daily dose of 120 mg/kg, plotted in Figure 4d. Average steady-state concentration was effectively identical across the three regimens, at 1.514, 1.513 and 1.512 mg/L, which is the same invariance seen in the single-dose sweep. Peak-to-trough behaviour was not. Immediate-release input at 40 mg/kg every 8 h gave a simulated steady-state peak of 3.163 mg/L against a trough of 0.235 mg/L, a fluctuation of 193.4 per cent. Gastroretentive input at 60 mg/kg every 12 h gave 2.073 and 0.781 mg/L, a fluctuation of 85.3 per cent. Gastroretentive input at 120 mg/kg every 24 h gave 2.378 and 0.643 mg/L, a fluctuation of 114.7 per cent. Accumulation ratios were 1.02, 1.00 and 1.00, so nothing accumulates on any of these schedules at this half-life.

Twelve-hourly gastroretentive input therefore delivered the same average exposure as three-times-daily immediate release on one fewer administration, with a peak 34.5 per cent lower and a trough 3.32 times higher.

3.9 Sensitivity: which parameter the answer depends on

Recomputing exposure at the limits of the reported parameter variability separates the two exposure metrics. Total exposure depends on clearance and on nothing else: varying clearance over its reported 52 per cent dispersion swung AUC(0-inf) by 142.5 per cent of the central value, from 31.54 to 9.96 mg.h/L, while varying the apparent volume or the absorption rate constant left it unchanged to within 0.03 per cent. The peak concentration depends chiefly on the apparent volume, which swung Cmax by 149.1 per cent, from 8.219 to 2.562 mg/L, against 39.7 per cent for clearance and 38.8 per cent for the absorption rate constant.

The formulation variable is thus the third most influential determinant of the peak and has no influence at all on total exposure, which is the quantitative form of the point made in Section 3.6.

4. Discussion

4.1 What the docking results say about the extract

The most reported constituent of licorice is not the one this analysis nominates. Glycyrrhizin dominates the literature on *Glycyrrhiza glabra* and dominates the root by mass, yet it could not be accommodated in either binding site: two poses and a positive score at the acid pump, two poses and a score of +25.61 kcal/mol at the cyclooxygenase channel. Its aglycone, generated in the gut by bacterial hydrolysis of the glucuronides, does better but still trails the flavonoids by roughly 5 kcal/mol at the pump and is excluded from cyclooxygenase-2 outright. The compounds that fit are the flavanones, isoflavans, chalcones and pterocarpans: glabridin, glabrene, liquiritin, liquiritigenin, formononetin, licochalcone A and glabranin.

Carbenoxolone provides an unusually informative control, because unlike a docking decoy it is a real drug with a known clinical history and a known mechanism. It was licensed for gastric ulcer and it is not an antisecretory agent; its activity is attributed to mucosal effects and to inhibition of 11beta-hydroxysteroid dehydrogenase, the same inhibition that produces the pseudoaldosteronism associated with licorice. A protocol that ranked carbenoxolone alongside vonoprazan at the proton pump would have been reporting something false about itself. It ranked it at -4.05 kcal/mol, 5.2 kcal/mol behind vonoprazan, which is the answer the pharmacology requires.

The size dependence in Figure 3d has a structural explanation rather than a statistical one. The vonoprazan site lies in a conduit the enzyme uses to admit cations from the gastric lumen, and the cyclooxygenase site is a narrow hydrophobic channel; neither is a shallow surface pocket that tolerates bulk. That both sites reject the same three compounds, and admit the same fourteen, is consistent with a genuine steric limit rather

than with a scoring artefact peculiar to one receptor.

4.2 What the exposure simulation adds that the formulation literature usually omits

The standard justification offered for a floating gastroretentive system is that gastric retention prolongs residence at the absorption site and therefore extends absorption. The simulation supports the second half of that claim and contradicts a common gloss on it. Under linear kinetics total exposure is set by dose and clearance, and no change in release rate altered it: AUC(0-inf) was 15.14 mg.h/L at every input rate from 1.1374 to 0.05 per hour. A gastroretentive carrier redistributes exposure. It does not create it. Claims that such a system increases bioavailability require an absorption-window or first-pass argument, and this model contains neither.

Once that is accepted, the design question becomes quantitative and has an answer. Time above the reference concentration peaked at an input rate of 0.20 per hour and then collapsed, reaching zero by 0.075 per hour. The mechanism of the collapse is visible in Figure 4a: past the optimum, the peak is flattened below the threshold faster than the curve is broadened above it. A carrier releasing with a nominal half-life much beyond four hours would, on these parameters, be worse than an immediate-release form on the very metric it was built to improve. This is not a conclusion available from a buoyancy measurement or a dissolution profile alone, and it is the argument for running the simulation before the formulation screen rather than after it.

The multiple-dose comparison points the same way with a different metric. Twelve-hourly gastroretentive input matched three-times-daily immediate release on average steady-state concentration while cutting fluctuation from 193.4 to 85.3 per cent. Notably the twenty-four-hourly regimen was worse than the twelve-hourly one on fluctuation, at 114.7 per cent, despite the slower input, because the longer interval more than offsets the flatter profile. Slower release and longer intervals are separate levers and they do not compose in the obvious direction.

4.3 The safety ceiling bounds the design from the other side

Prolonged systemic exposure to glycyrrhizin and its metabolites is not a neutral objective. Licorice-induced pseudoaldosteronism is dose and duration dependent, and Japanese Kampo labelling treats a daily intake at or above 2.5 g of licorice as contraindicated in patients with aldosteronism, myopathy or hypokalaemia; in elderly patients given a preparation containing 6.0 g of licorice for longer than thirty days, more than 80 per cent developed pseudoaldosteronism or related symptoms including hypokalaemia [14]. Oral bioavailability of glycyrrhizin itself is low, reported as under 4 per cent in the rat and not detectable in humans [13], so systemic exposure after an oral dose is largely exposure to the aglycone generated by gut microbial hydrolysis.

Two consequences follow for a gastroretentive design. A carrier that succeeds in flattening the

profile raises the trough, and it is trough concentration over time rather than peak concentration that the pseudoaldosteronism literature associates with risk. And the constituents this analysis nominates as the likely site-engaging fraction are the flavonoids, not the saponin, which suggests that a deglycyrrhizinated extract is the more rational starting material for a formulation of this kind. That inference is a hypothesis generated by the docking, not a demonstrated fact, and it is exactly the sort of claim a comparative in vitro assay would settle quickly.

4.4 Limitations

The docking limitations are specific rather than generic. Both receptors were rigid, so induced fit was not sampled, and a site that opens on ligand binding will be scored as more exclusive than it is; that caveat applies with most force to the three triterpenoids, whose exclusion is a statement about the deposited conformation and not about the protein in solution. The scoring function ranks better than it quantifies, so the 0.45 kcal/mol spread across the top three constituents at the acid pump does not order them. The proton pump structure is the porcine enzyme, the only gastric H+/K+-ATPase for which a ligand-bound luminal-open structure exists, and although the site is highly conserved the transfer to the human enzyme is an assumption. Removing the cobalt protoporphyrin from cyclooxygenase-2 was necessary and is justified by its distance from the docking site, but it is a modification of the deposited structure. One residue was deleted from the proton pump to remove a bond that the deposited model's chain break had created artefactually.

The pharmacokinetic limitations are heavier. The parameters describe Sprague-Dawley rats after a single oral dose and are not human parameters; the numerical values above should be read as the behaviour of a model rat, and the transferable finding is the shape of the input-rate relationship rather than any particular concentration. Oral bioavailability was not reported in the source, so every concentration is apparent. The source's own reported clearance could not be reconciled with its reported dose and AUC, and clearance was therefore recomputed from the primary quantities, a decision stated in Section 2.6 that another analyst might make differently. Linear kinetics was assumed throughout, which is what allows superposition and what makes total exposure invariant; if the disposition of this compound is saturable at the doses simulated, that invariance fails. The model does not capture enterohepatic recycling, and the 40.8 per cent underestimate of the observed peak is the visible cost of that omission. The reference concentration used to define time above threshold is internal to the simulation and carries no pharmacodynamic meaning; a threshold anchored on a measured effect concentration would change the position of the optimum, though not the fact that one exists.

Finally, the whole study is a set of computational predictions. No compound was shown to bind anything, no formulation was prepared, and no concentration was measured.

4.5 What would settle this

Three experiments would convert most of the above into evidence, and they are named here as the work the field should now do rather than as promises.

The first is a comparative inhibition assay of glabridin, glabrene and liquiritin against gastric H+/K+-ATPase in isolated vesicles, with vonoprazan as the positive control and glycyrrhizin as the negative. That directly tests the paper's central ranking, including the prediction that the saponin is inactive at this target, and it is a week of bench work.

The second is a deglycyrrhizinated versus whole-extract comparison in a standard gastric ulcer model. The docking predicts that removing glycyrrhizin should not reduce activity at these two targets, which is a falsifiable claim and one with direct formulation consequences.

The third is a floating microsphere batch series formulated deliberately across the release-rate range identified here, from a nominal input half-life of about one hour to about ten, characterised by in vitro release and then by in vivo exposure. The simulation predicts a non-monotonic relationship with an optimum near 3.5 h. A batch series that found the optimum elsewhere would locate the error in the model, and a batch series that found no optimum at all would refute the premise.

5. Conclusion

Within the limits of a rigid-receptor docking protocol validated at 0.553 and 0.482 angstroms against its own crystallographic controls, the constituents of *Glycyrrhiza glabra* root that plausibly engage the gastric acid pump and the cyclooxygenase channel are the flavonoids rather than glycyrrhizin, which neither site could accommodate. Under a one-compartment model built from published rat exposure data, gastroretentive sustained input redistributes exposure without increasing it, and does so usefully only within a bounded range of release rates, with an optimum near an input half-life of three and a half hours on these parameters. A floating microsphere designed for this extract therefore has a target release rate rather than an instruction to release as slowly as possible, and a rational starting material that may not be the whole root extract. Both conclusions are computational predictions and require experimental confirmation.

Declarations

Ethics approval. This study was conducted entirely in silico using published structural and pharmacokinetic data.

Competing interests. The authors declare no competing interests.

Funding. No funding was received for this work.

References

1. Xie X, Ren K, Zhou Z, Dang C, Zhang H. The global, regional and national burden of peptic ulcer disease from 1990 to 2019: a population-based study. BMC Gastroenterol. 2022;22:58. doi:10.1186/s12876-022-02130-2

2. Wahab S, Annadurai S, Abullais SS, Das G, Ahmad W, Ahmad MF, et al. Glycyrrhiza glabra (licorice): a comprehensive review on its phytochemistry, biological activities, clinical evidence and toxicology. Plants. 2021;10(12):2751. doi:10.3390/plants10122751

3. Abe K, Irie K, Nakanishi H, Suzuki H, Fujiyoshi Y. Crystal structures of the gastric proton pump. Nature. 2018;556(7700):214-218. doi:10.1038/s41586-018-0003-8

4. Orlando BJ, Malkowski MG. Crystal structure of rofecoxib bound to human cyclooxygenase-2. Acta Crystallogr F Struct Biol Commun. 2016;72(Pt 10):772-776. doi:10.1107/S2053230X16014230

5. Kawashima Y, Niwa T, Takeuchi H, Hino T, Itoh Y. Hollow microspheres for use as a floating controlled drug delivery system in the stomach. J Pharm Sci. 1992;81(2):135-140. doi:10.1002/jps.2600810207

6. Lipinski CA, Lombardo F, Dominy BW, Feeney PJ. Experimental and computational approaches to estimate solubility and permeability in drug discovery and development settings. Adv Drug Deliv Rev. 1997;23(1-3):3-25. doi:10.1016/S0169-409X(96)00423-1

7. Veber DF, Johnson SR, Cheng HY, Smith BR, Ward KW, Kopple KD. Molecular properties that influence the oral bioavailability of drug candidates. J Med Chem. 2002;45(12):2615-2623. doi:10.1021/jm020017n

8. Egan WJ, Merz KM Jr, Baldwin JJ. Prediction of drug absorption using multivariate statistics. J Med Chem. 2000;43(21):3867-3877. doi:10.1021/jm000292e

9. Ghose AK, Viswanadhan VN, Wendoloski JJ. A knowledge-based approach in designing combinatorial or medicinal chemistry libraries for drug discovery. 1. A qualitative and quantitative characterization of known drug databases. J Comb Chem. 1999;1(1):55-68. doi:10.1021/cc9800071

10. Trott O, Olson AJ. AutoDock Vina: improving the speed and accuracy of docking with a new scoring function, efficient optimization, and multithreading. J Comput Chem. 2010;31(2):455-461. doi:10.1002/jcc.21334

11. Eberhardt J, Santos-Martins D, Tillack AF, Forli S. AutoDock Vina 1.2.0: new docking methods, expanded force field, and Python bindings. J Chem Inf Model. 2021;61(8):3891-3898. doi:10.1021/acs.jcim.1c00203

12. Zhou N, Zou C, Qin M, Li Y, Huang J. A simple method for evaluation pharmacokinetics of glycyrrhetinic acid and potential drug-drug interaction between herbal ingredients. Sci Rep. 2019;9:11480. doi:10.1038/s41598-019-47880-4

13. Xu R, Liu X, Yang J. A semi-physiologically based pharmacokinetic pharmacodynamic model for glycyrrhizin-induced pseudoaldosteronism and prediction of the

dose limit causing hypokalemia in a virtual elderly population. PLoS One. 2014;9(12):e114049. doi:10.1371/journal.pone.0114049

14. Yoshino T, Shimada S, Homma M, Makino T, Mimura M, Watanabe K. Clinical risk factors of licorice-induced pseudoaldosteronism based on glycyrrhizin-metabolite concentrations: a narrative review. Front Nutr. 2021;8:719197. doi:10.3389/fnut.2021.719197
15. Bickerton GR, Paolini GV, Besnard J, Muresan S, Hopkins AL. Quantifying the chemical beauty of drugs. Nat Chem. 2012;4(2):90-98. doi:10.1038/nchem.1243
16. Semwal DK, Kumar A, Semwal RB, Dadhich NK, Chauhan A, Kumar V. Glycyrrhizin (glycyrrhizic acid): pharmacological applications and associated molecular mechanisms. Drugs Drug Candidates. 2025;4(4):44. doi:10.3390/ddc4040044
17. Yan M, Fang PF, Li HD, Xu P, Liu YP, Wang F, et al. Lack of effect of continuous glycyrrhizin administration on the pharmacokinetics of the P-glycoprotein substrate talinolol in healthy volunteers. Eur J Clin Pharmacol. 2013;69(3):515-521. doi:10.1007/s00228-012-1391-6